

# PRELIMINARY SIMULATIONS ON CHIRP-LESS BUNCH COMPRESSION USING DOUBLE-EEX BEAMLINE

Gwanghui Ha, Pohang Accelerator Laboratory, Pohang, Gyeongbuk 790-784, KOREA  
John Gorham Power, Manoel Conde, Darrell Scott Doran, and Wei Gai, Argonne National Laboratory, Argonne, IL 60439, USA

## Abstract

An emittance exchange (EEX) beamline can be used to compress an electron bunch via its transverse-to-longitudinal exchange mechanism. We are investigating this as an alternative to the normal magnetic chicane bunch compressor. The chicane method requires a longitudinal chirp before the chicane (since it relies on the path length difference of different energies) which results in an unwanted chirp after the compressor. Alternatively, the EEX method uses quadrupole magnets to compress the bunch. In this paper, we present preliminary simulations in preparation for a demonstration of chirp-less bunch compression using an EEX beamline at the Argonne Wakefield Accelerator facility.

## INTRODUCTION

The upgrade of the single emittance exchange (EEX) beamline to a double-EEX beamline is underway at the Argonne Wakefield Accelerator (AWA) facility. One of the first experiments planned for the double-EEX beamline is to use it as a bunch compressor [1]. Transverse beam manipulations control the longitudinal properties downstream of the EEX beamline [2] because the EEX beamline exchanges the longitudinal and transverse phase space. We are exploring whether this exchange based compression method can provide benefits compared to a magnetic chicane compressor [3].

The magnetic chicane compressor is well understood and is currently used in most state-of-the-art accelerators [3-5]. However, the chicane compressor is known to have two limitations. First, the chicane compressor requires an energy chirp before the compressor and therefore an energy de-chirping process afterward. A linear chirp allows the tail of the bunch to catch up with its head due to the path length differences inside the chicane. De-chirping is needed afterward to remove the unwanted chirp for the application. Second, the bunch acquires a double-horn current profile after the chicane compression when the compression is strong [3], and this high peak current can lead to emittance growth [6].

The EEX compressor uses a different principle for the compression than a chicane compressor and avoids the two limitations of the chicane-compressor. First, the EEX compressor focuses the bunch horizontally to compress it longitudinally and therefore does not require a chirp. Second, due to its different operating principle, a double-horn shape does not appear on the final current profile even when the compression is strong. Finally, we note that the EEX beamline can be used to manipulate all

longitudinal properties. Therefore, it can control the energy chirp and, when used with a mask, the current profile shape too [2].

In this paper, we show preliminary simulation results for the planned demonstration of bunch compression using a double-EEX beamline at the AWA facility. All simulation of the double-EEX beamline (Fig. 1) were performed with the particle tracking code GPT [7], including 3D space-charge [7] and 1D CSR [8]. A 6D Gaussian bunch was generated at the entrance to the beamline and GPT was used to track the particles through the beamline. We numerically study the control of the bunch length in the first section of the paper and control of the chirp in the second. In the last section, we discuss the emittance growth due to coherent synchrotron radiation (CSR) which appears to be a serious limitation of this method.

## DOUBLE EEX FOR BUNCH COMPRESSION

Double-EEX exposes the longitudinal phase space of the bunch in the middle section between the two stages of EEX where we can tailor the longitudinal phase space by simple manipulations on the transverse phase space. The double-EEX configuration (Fig. 1) consists of two double-dogleg EEX beamlines made from two identical doglegs with a transverse deflecting cavity (TDC) in the middle [9]. Here we added two more quadrupole magnets before and after each single EEX beamline to adjust the top-right and bottom-left of the transport matrix of each single EEX beamline. The first EEX beamline rotates the initial longitudinal phase space to transverse space in the middle where it has a long bunch length for a weak CSR at the second EEX and a small beam size for the short bunch at the end. The compression ratio ( $\sigma_{z,i}/\sigma_{z,f}$ ) can be adjusted with the quadrupoles in the middle of the beamline. The second EEX beamline rotates the phase spaces back to their original spaces but with a different bunch length.

## CONTROL OF THE BUNCH LENGTH

The quadrupoles in the middle section of the double EEX beamline can be used to control the bunch length after the beamline. The beamline and initial beam parameters are given in Table 1. The third quadrupole in the middle section was varied to adjust the bunch compression and expansion.



Figure 1: Schematic diagram showing EEX compressor. Each EEX beamline consists of two identical dogleg, deflecting cavity, and four quadrupoles.

Table 1: Beamline and Initial Beam Parameters

Beamline parameters	Value	Unit
Bending angle	20	degree
Dipole-to-Dipole	2	M
Dispersion of dogleg	0.88	M
TDC kick strength	1.1	m <sup>-1</sup>
Beam parameters	Value	Unit
Energy	50	MeV
Charge	100	pC
$\sigma_x$	1	Mm
$\sigma_y$	1	Mm
$\sigma_z$	0.7	Mm
$\sigma_{xx'}/\sigma_x^2$	-0.2	m <sup>-1</sup>
$\sigma_{yy'}/\sigma_y^2$	0.0	m <sup>-1</sup>
$\sigma_{zz'}/\sigma_z^2$	0.0	m <sup>-1</sup>

Figure 2 shows the final rms bunch length for different quadrupole strengths. The orange line (0.7 mm) is the initial bunch length. When the quadrupole strength is -1.4 T/m, the final bunch length is equal to the initial bunch length. A weaker quadrupole generates a longer bunch length (expansion) and a stronger quadrupole generates a shorter bunch (compression). The value of the minimum bunch length is limited by the emittance, space-charge, and CSR. In this case, the minimum bunch length is ~25 micron. Note, the bunch length after BC2 of LCLS is ~20 micron [3].

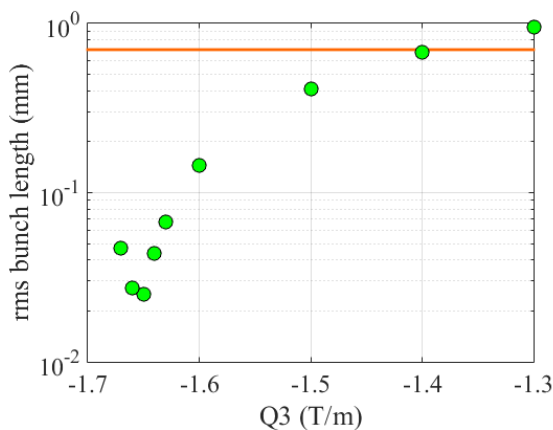


Figure 2: The final rms bunch length at the end of double-EEX beamline. Q3 is the strength of the third quadrupole magnet in the middle section. Orange line shows the initial bunch length (0.7 mm), and green dots correspond to the bunch length for each quadrupole strength.

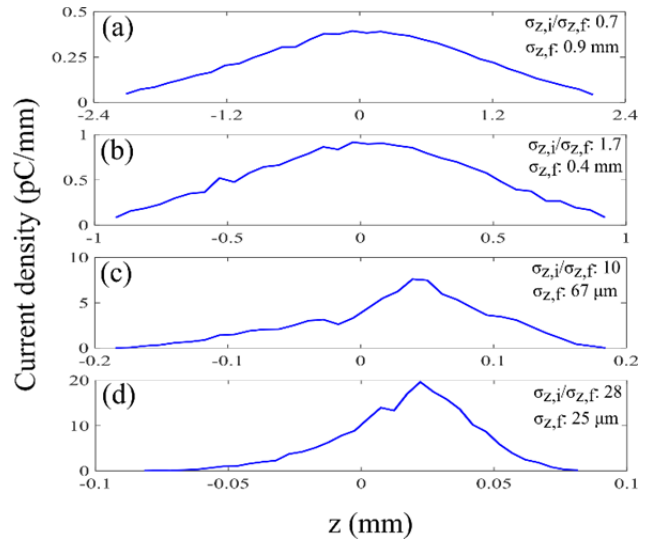


Figure 3: Current profiles at the end of double-EEX beamline for an initial rms bunch length of 0.7 mm. Each figure corresponds to each Q3 strength. Q3 strengths for each case are (a) -1.3 T/m, (b) -1.5 T/m, (c) -1.63 T/m, and (d) -1.65 T/m. Here the positive z is the head.

Figure 3 shows the final current profile for several of the cases in Fig. 2. These results show that symmetric current profiles are achievable for all of the compression ratios. Especially, Fig. 3 (d) shows a strong compression case whose bunch length is changed from 0.7 mm to 0.025 mm (i.e. compression ratio of 28). The head and the tail are elongated compared to a long bunch cases in Fig. 3, but it does not have double horned feature that is commonly observed after the chicane compressor [3].

### CONTROL OF THE CHIRP

The quadrupoles in the middle section of the double EEX beamline can also be used to control the chirp after the beamline. To demonstrate the chirp control capability, the third and fourth quadrupoles in the middle section were used to change the chirp while preserving the bunch length. Table 2 shows the quadrupole settings and expected final chirps. Here we use a moderate compression ratio of 3.5 which is similar to the ratio used in the first bunch compressor in many XFELs. The final bunch length is 0.2 mm.

Figure 4 shows the longitudinal phase spaces after the double-EEX beamline. Each case in this figure corresponds to the quadrupole settings of Table 2. The final chirp for each of these cases are (a) -0.8 m<sup>-1</sup>, (b) -4.0 m<sup>-1</sup>, (c) -7.6 m<sup>-1</sup>, (d) 15.2 m<sup>-1</sup>, (e) 18.8 m<sup>-1</sup>, and (f) 21.9 m<sup>-1</sup>.

These results clearly show that the chirp can be varied from negative to positive while preserving the bunch length.

Table 2: Middle quadrupole setting and corresponding final chirp. Q3 and Q4 are the third and the fourth quadrupole strengths in the middle section.

Q3	Q4	Estimated final chirp
-2.2 T/m	5.48 T/m	-1.88 m <sup>-1</sup>
-1.9 T/m	3.11 T/m	-5.07 m <sup>-1</sup>
-1.6 T/m	1.71 T/m	-8.50 m <sup>-1</sup>
-2.2 T/m	4.58 T/m	14.65 m <sup>-1</sup>
-1.9 T/m	2.43 T/m	18.14 m <sup>-1</sup>
-1.6 T/m	1.16 T/m	21.19 m <sup>-1</sup>

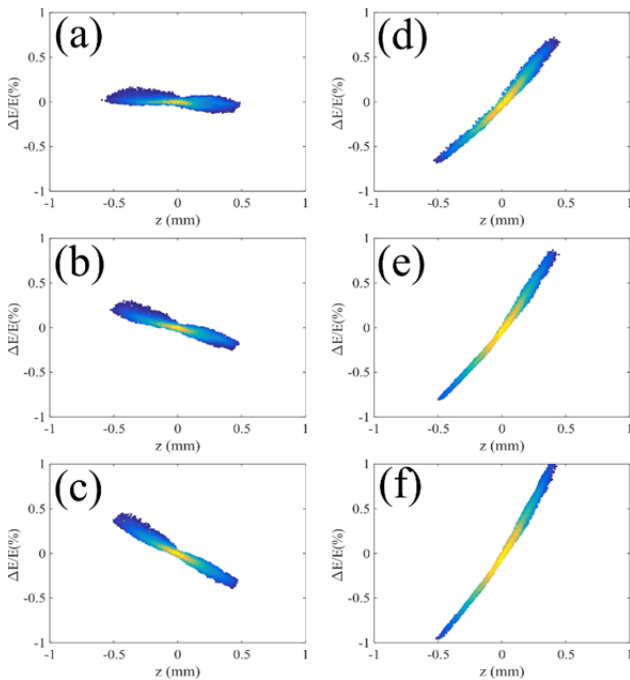


Figure 4: Longitudinal phase spaces at the end of double-EEX beamline. Each case corresponds to different Q3 and Q4 settings.

## CSR AND EMITTANCE GROWTH

The study of the EEX compressor method has so far focused on its advantages (compression and chirp control) while ignoring its disadvantages. However, the eight dipole magnets composing the double-EEX beamline can cause a serious emittance growth due to CSR. CSR is strong in our case due to our bending angle of 20 degrees. Figure 5 shows the horizontal emittance at the end of the beamline. It starts from 1 micron and increases to 5-10 microns due to CSR.

Since horizontal and longitudinal phase spaces are entangled and disentangled while the beam travels the double-EEX beamline, CSR directly (change energy) and indirectly (via dispersion) affects both phase space planes. Therefore, mitigation of CSR in the EEX beamline may require different approaches compared to the chicane-type

compressor. CSR study on EEX beamline will be the subject of our next work and we are actively seeking ways to suppress it.

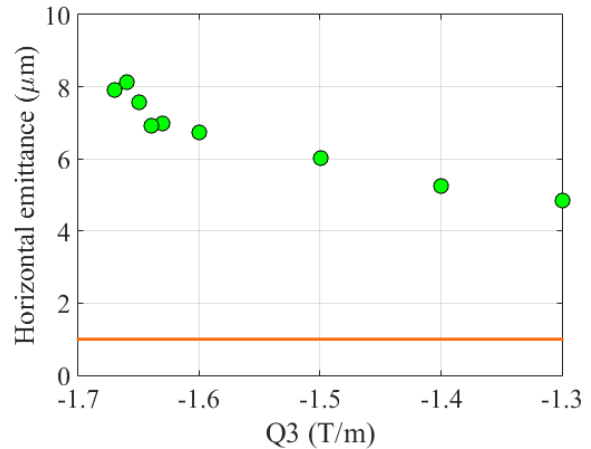


Figure 5: Final horizontal emittance corresponding to different Q3 strengths. The initial emittance (orange line) is 1 micron (normalized).

## REFERENCES

- [1] A. A. Zholents and M. S. Zolotarev, ANL-APS-LS-327 (2011).
- [2] G. Ha *et al.*, Phys. Rev. Lett. 118, 104801 (2017).
- [3] LCLS Conceptual design report.
- [4] [xfel.riken.jp/eng/](http://xfel.riken.jp/eng/)
- [5] Pohang XFEL Conceptual design report.
- [6] T. K. Charles *et al.*, Phys. Rev. Accel. Beams 20, 030705 (2017).
- [7] [www.pulsar.nsl/gpt](http://www.pulsar.nsl/gpt)
- [8] I. Bazarov and T. Miyajima, in Proc. of EPAC08, p118 (2008).
- [9] P. Emma *et al.*, Phys. Rev. Accel. Beams 9, 100702 (2006).